UDC 546.05-666.651

D0I: 10.15372/CSD20180204

Synthesis and Properties of Al_2O_3–Fe_2O_3 Ceramic Composite with Limited Electrical Conductivity

G. R. KARAGEDOV[1], A. A. KRASNOV[2,3], A. E. LEVICHEV[2], E. V. MAMOSHKINA[2]

[1]Institute of Solid State Chemistry and Mechanochemistry, SB RAS,
Novosibirsk, Russia

E-mail: garik@solid.nsc.ru

[2]Institute of Nuclear Physics, SB RAS,
Novosibirsk, Russia

[3]Novosibirsk State University,
Novosibirsk, Russia

(Received November 16, 2017)

Abstract

Ceramic materials with a density of more than 95 % of theoretical containing 1–30 mass % of iron oxide were synthesized in the Al_2O_3–Fe_2O_3 system. During ceramics air sintering, the material with Fe_2O_3 content below 10 % is monophase and comprises α-Al_2O_3-based solid solution. With Fe_2O_3 concentration above 10%, an iron oxide-based solution is generated in significant amounts. As soon as the material becomes two-phase, the value of its electrical conductivity increases by three orders of magnitude and reaches 10^{-8}–10^{-9} Sm/m. Iron oxide is reduced to metal when trying to increase material density by vacuum sintering or hot isostatic pressing. Furthermore, a composite representing uniformly distributed spherical metallic iron particles in the α-Al_2O_3 matrix is generated.

Keywords: alumina, ceramics, composite, electrical conductivity

INTRODUCTION

In composite materials, properties of their components are often combined. Owing to which, the former have unique characteristics, unachievable by other means. For example, a material comparable according to mechanical properties and mechanical properties and radiation and chemical resistance with ceramics made of alumina but simultaneously notable for the significant electrical conductivity is required in some cases. This task has been solved by introducing carbon nanotubes (CNT) into the alumina matrix [1, 2]. However, for a number of practically important tasks, for example, for injectors of accelerators or vacuum waveguide microwave windows, the electrical conductivity of the material should not exceed 10^{-5} S/m, so that while maintaining insulating properties it can ensure accumulated charges leaking leading to ceramics breakdown and destruction. Unfortunately, conductivity versus the content of nanotubes is of a percolation transition and composite conductivity changes skippingly from 10^{-12} to 10^{-1} S/m with an increase in the concentration of CNT from 1 to 1.2 % [2] or from 10^{-8} to 10^{-1} S/m depending on the method of consolidation [1].

This work made an attempt to solve this task by replacing a portion of Al^{3+} cations for Fe^{3+}, taking into account that oxides of these metals have the same structure and form solid solutions between themselves [3], while electrical conductivity of Fe_2O_3 at room temperature is 10^{-5} S/m [4].

Furthermore, when developing materials with the above electroconductive properties, it has to be taken into account that the density of the resulting ceramics should be maximally close to theoretical to ensure leakage level of no more than 10^{-10} (L · Torr)/s.

EXPERIMENTAL

The work used α-Al_2O_3 powder synthesized by the technique [5, 6], with an average particle size of 100 nm; fine-dispersed aluminium hydroxide (Basel-Cement CJSC, TU 1711-046-00196368-95); extra pure iron oxide (Donetsk plant of chemical reagents, TU 6-09-1418-78) with dimensions of crystallites of 120 nm.

Moulding powders were prepared by three methods.

Method 1. The calculated amount of iron oxide and 3 % nanopowder [7] was introduced into aluminum nitrate solution (per the final product) as a seeding agent. Ammonia was added dropwise by drop with vigorous stirring and the gel was precipitated. The resulting gel was aged for 24 h, air dried at 500 °C and then calcined at 950 °C.

Method 2. A dry mixture of aluminum hydroxide with 4 % nanopowder and the computed amount of iron oxide was treated in an AGO-2M planetary mill with an acceleration of 10*g* for 15 min using grinding balls with a diameter of 5 mm and drums made of ZrO_2 and then calcined at 950 °C.

Method 3. Alpha alumina (α-Al_2O_3) powders (100 nm) with the calculated amount of Fe_2O_3 were jointly were ground in an agate mortar.

Prior to pressing, the powders produced by methods 1 and 2 were dispersed using an AGO-2M mill with an acceleration of 10*g* for 5 min using grinding balls with a diameter of 3 mm and drums made of ZrO_2. Moulding pills with a diameter of 16 mm and a height of 3–4 mm and bars with a size of 40 × 40 × 5 mm was carried out by dry uniaxial pressing near 30 MPa pressure followed by isostatic compression near 200–250 MPa pressure using an AIP3-12-60C device (American Isostatic Press, USA). In some cases, cylinders with a diameter and a height of 25 mm were moulded.

After pressing, the samples were air sintered in THE Lac 04/17 furnace for 1.5 h, then some of them were baked in the vacuum furnace SNVE (Prisma LLC, Russia) near 10^{-6} mm Hg pressure. Hot isostatic pressing (HIP) of pre-sintered samples was carried out using AIP6-30N unit in a graphite furnace for 1 h near 200 MPa argon pressure.

The density of the resulting ceramics was determined geometrically or by the method of Archimedes according to GOST 20018-74.

X-ray phase analysis of powders, sintered materials, and crystallite size determination was carried out using the DRON-4 X-ray diffractometer with Cu$K_{\alpha 1}$-radiation and a graphite monochromator, and also the Bruker D8 Advance diffractometer. The sizes of crystallites in powders and grains in sintered materials were determined using PowderCell 2.4 or Topas software with the obligatory introduction of standard parameters of samples obtained under identical shooting conditions. The results for both softwares are in agreement with an accuracy up to nm units and are given in the text with rounding up to tens of nanometers.

Electrical conductivity after the vacuum deposition of the gold layer (~25 nm) was measured at a constant current at a voltage of 10 V using the Keithley 6485 picoammeter (USA). Polarization phenomena were observed for a number of samples (Fig. 1), therefore the values acquired after 3 s after the voltage was taken at the different polarity and averaged. Although the specific resistance values given in the paper can be considered as approximate, the observed effects far exceed the possible inaccuracies in their determination.

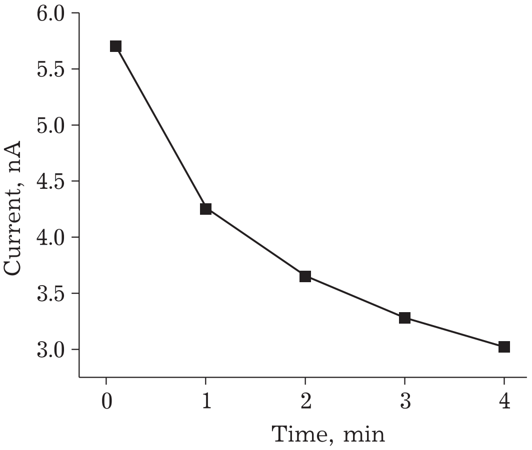

Fig. 1. Changes of the strength of the constant current passing through a sample with Fe_2O_3 content of 20 % over time.

Electron microscopy images and EDS data were received using the JEOL JSM 6460LV microscope.

RESULTS AND DISCUSSION

As traditional alumina ceramics sintering up to high densities requires temperatures of 1700–1800 °C, and iron oxides are unstable under these conditions, therefore the selection of the initial components is limited by ultrafine powders. Regardless of the preparation method of initial powders for moulding used in the work, all of them are ultrafine. In case of grinding in the mortar of aluminum and iron oxides with dimensions of about 0.1 μm, this is obvious, and when two other methods are used, this is anticipated, since without the addition of iron oxide, α-Al_2O_3 nanopowder is obtained in both cases [6, 8]. Figure 2 presents the SEM image of 5 % Fe_2O_3 containing powders obtained by method 1 as confirmation. Figure 3 gives the X-ray diffraction patterns of 5 % Fe_2O_3 containing powders synthesized according to methods 1 and 2. The first one is presented by only two sets of peaks corresponding to the phases with the structure of corundum and hematite with crystallite size of 110 and 120 nm, respectively, i.e. iron oxide particles have not changed during the preparation of the powder, and α-Al_2O_3 particles were ultimately formed from aluminium nitrate solution.

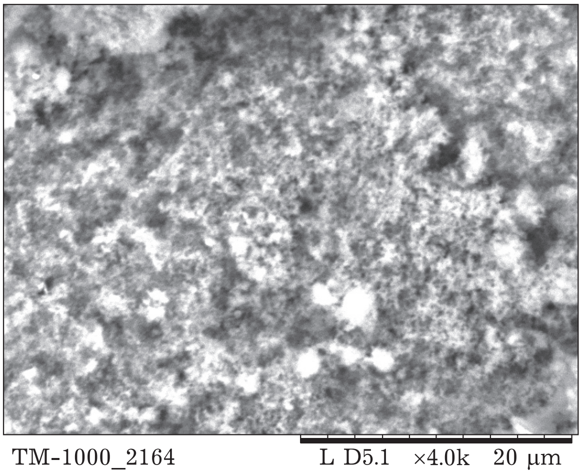

Fig. 2. SEM of 5 % Fe_2O_3 containing powder synthesized according to method 1.

In the second case, iron oxide peaks are barely visible, and phase peaks with the structure of α-Al_2O_3 (corundum) with a size of crystallites of 90 nm are shifted to the area of smaller interplane distances by about 0.12 %, which corresponds to the formation of a solid solution. Thus, during mechanochemical treatment of a mixture of $Al(OH)_3$ and Fe_2O_3, close contact between the reagents, facilitating the diffusion of ions in the subsequent perforation emerges even under adopted soft conditions, although it is impossible to exclude

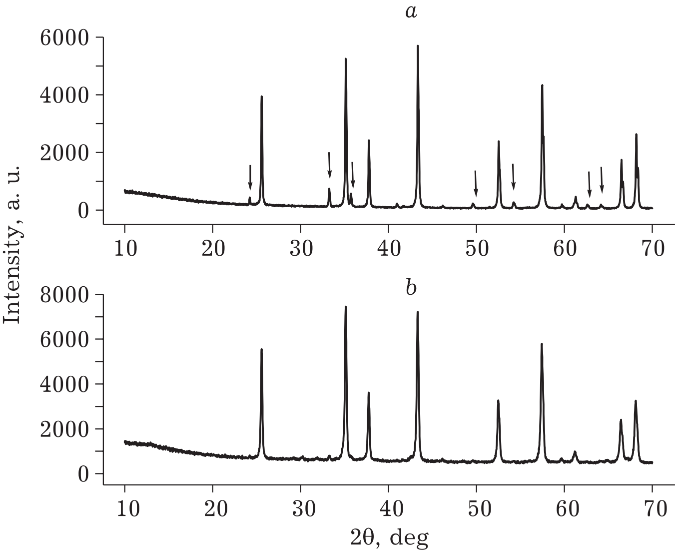

Fig. 3. X-ray diffraction patterns of 5 % Fe_2O_3 containing powders synthesized according to methods 1 (a) and 2 (b). Arrows indicate peaks attributed to Fe_2O_3.

TABLE 1

Density (ρ) and electrical conductivity (σ) of air-sintered materials

Fe_2O_3 content, %	Method	$\rho_{1350,g}$, g/cm^3	$\rho_{1500,g\ (A)}$, g/cm^3	$\rho_{1500,\ A}$, %	σ_{1350}, S/m	σ_{1500}, S/m
1.0	2	–	3.72 (3.80)	94.8	–	$<10^{-11}$
3.0	2	–	3.79 (3.86)	95.8	–	$<10^{-11}$
4.5	2	–	3.84 (3.91)	96.5	–	$4\cdot10^{-11}$
4.5	2	–	3.83 (3.85)	–	–	$3\cdot10^{-11}$
5.0	2	–	3.83 (3.95)	97.5	–	$3.5\cdot10^{-12}$
5.0	1	3.79	3.84 (3.85)	95.1	–	$<1.5\cdot10^{-12}$
5.0	3	–	3.81 (3.89)	96.0	–	$<3.5\cdot10^{-12}$
9.1	1	–	3.71 (3.79)	92.4	–	–
10	3	3.84	3.87 (3.90)	95.1	$1.5\cdot10^{-11}$	$<10^{-11}$
15	3	3.87	3.89	–	$4\cdot10^{-9}$	–
20	3	3.84	3.92 (3.94)	93.8	$2.5\cdot10^{-8}$	$1.5\cdot10^{-8}$
20 (bar)	3	3.81	–	–	$3.5\cdot10^{-8}$	–
20 (cylinder)	3	3.79	3.84 (3.92)	93.3	–	$2\cdot10^{-8}$
30	3	3.94	3.97 (4.06)	94.2	$3.5\cdot10^{-8}$	–
30[a]	2	3.95	–	–	$7.5\cdot10^{-11}$	–

Note. 1. $\rho_{1350,g}$ is geometric density of materials sintered at 1350 °C; $\rho_{1500,g\ (A)}$ is geometric density (g) and solidness determined by the method of Archimedes (A) of materials sintered at 1500 °C; $\rho_{1500,\ A}$ is percentage of the theoretically possible. 2. σ_{1350} and σ_{1500} are electrical conductivities of materials sintered at 1350 and 1500 °C, respectively.

[a] Without addition of inoculating particles.

the mutual dissolution of the reagents already in the drum of the mill.

Table 1 gives the data on the density and electrical conductivity of air-sintered materials. The theoretical density was computed in the approximation that the density of a solid solution is not different from that of the main component and therefore is of estimative nature.

It is worth noting that with increasing air-sintering temperature from 1350 to 1500 °C, material density generally increases by 2–3 %. However, subsequent vacuum heating at 1500 and even 1600 °C and simultaneous using temperature and pressure (GIP), do not lead to a further increase in density.

Regardless of the preparation method of the pressed powder, after air sintering, X-ray diffraction patterns of materials containing less than 10 % Fe_2O_3 are presented only by reflections relating to the phase with corundum structure. The X-ray diffraction patterns of materials that contain more than 10 % of Fe_2O_3, simultaneously identify phases on the ground of corundum and hematite. Moreover, the peaks of the different phases are clearly shifted to the opposite direction (Fig. 4) as compared to their position for pure oxides. Obviously, Fe^{3+} cations replace Al^{3+} in the corundum lattice, and Al^{3+} species – Fe^{3+} in the hematite lattice. This fact is in agreement with the phase diagram of the Al_2O_3–Fe_2O_3 system [3], from which it follows that with iron oxide (III) content up to 10 mass %, only one solid solution with the corundum structure is formed, and at 15 % Fe_2O_3 and more, if not to use methods of quenching from high temperatures, there should also be a phase based on hematite. At 1500 °C, a phase with the spinel structure should also appear in the system, however, during cooling, it manages to transform into a solution with hematite structure.

The second phase does not appear in electron microscopic images of composite ceramics sintered at 1350 °C (Fig. 5) with Fe_2O_3 content of 10 %, and the material is unambiguously two-phase with 15 % of iron (III) oxide. As demonstrated by EDS analysis, light areas contain much more iron than dark ones.

The appearance of the phase with the structure of hematite, which has a significantly higher electrical conductivity, in ceramic samples leads to the fact that electrical

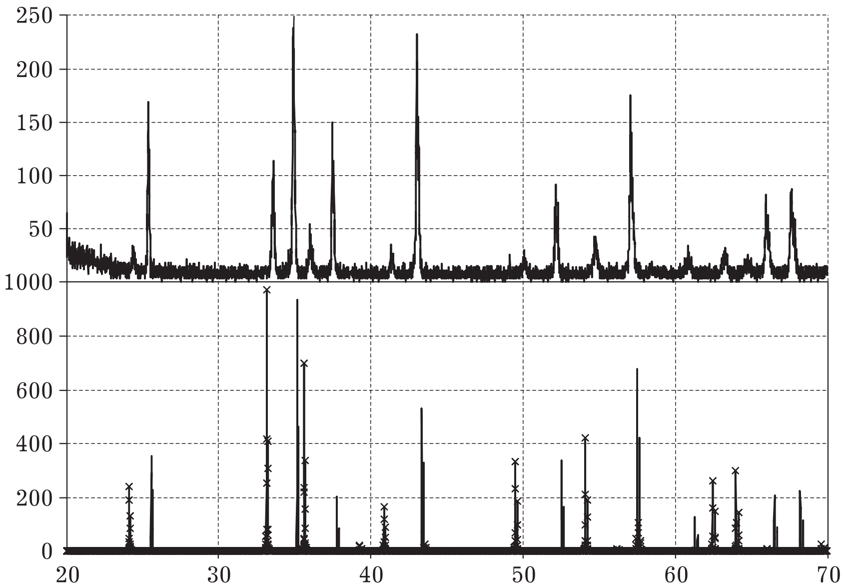

Fig. 4. X-ray diffraction pattern of 30 % Fe_2O_3 containing material air-sintered at 1350 °C. Lines below indicate peaks positions of pure oxides; × is Fe_2O_3.

conductivity of the composite increases by three orders of magnitude (see Table. 1). For samples with iron oxide content of over 15 %, electrical conductivity is 10^{-8}–10^{-9} S/m, and in case of 1^{-10} % of Fe_2O_3 it varies within 10^{-11}–10^{-12} S/m. As can be seen from the data in Fig. 5, already with 15 % Fe_2O_3, the amount of the phase with hematite structure is significant and it can fairly generate a three-dimensional closed grid resulting in a steplike increase in electrical conductivity.

At the same time, as it follows from the data of Table 1, the material obtained by method 1 but without the introduction of seed particles does not have the required electrical conductivity, despite a significant content of Fe_2O_3 therein. It is obvious that ultrafine α-Al_2O_3 particles are not generated without the introduction of a seed, and those produced during sintering at higher temperatures are less reactive. The reflections corresponding to a solid solution with the hematite structure in the X-ray diffraction pattern of the material are hardly visible. Perhaps active small particles of hematite have time to dissolve in large α-Al_2O_3 particles, and the opposite process is much slower. The amount of solution with hematite structure that managed to form

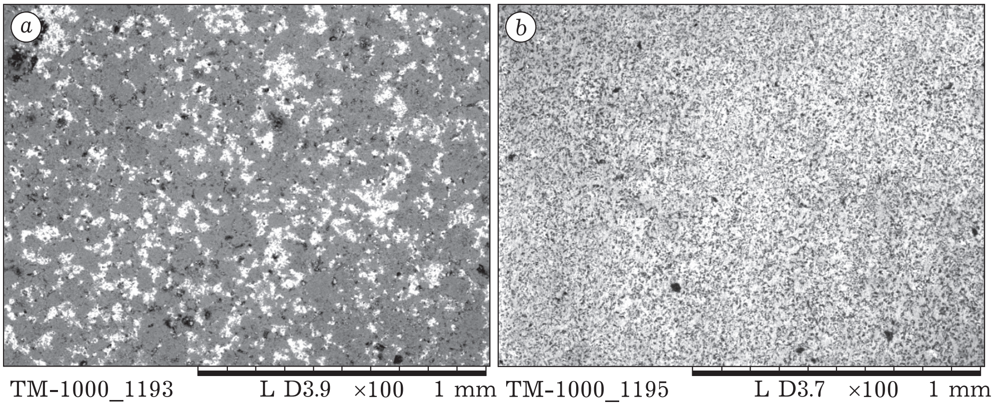

Fig. 5. SEM image of air-sintered at 1350 °C material containing of 15 (*a*) and 10 % (*b*) Fe_2O_3.

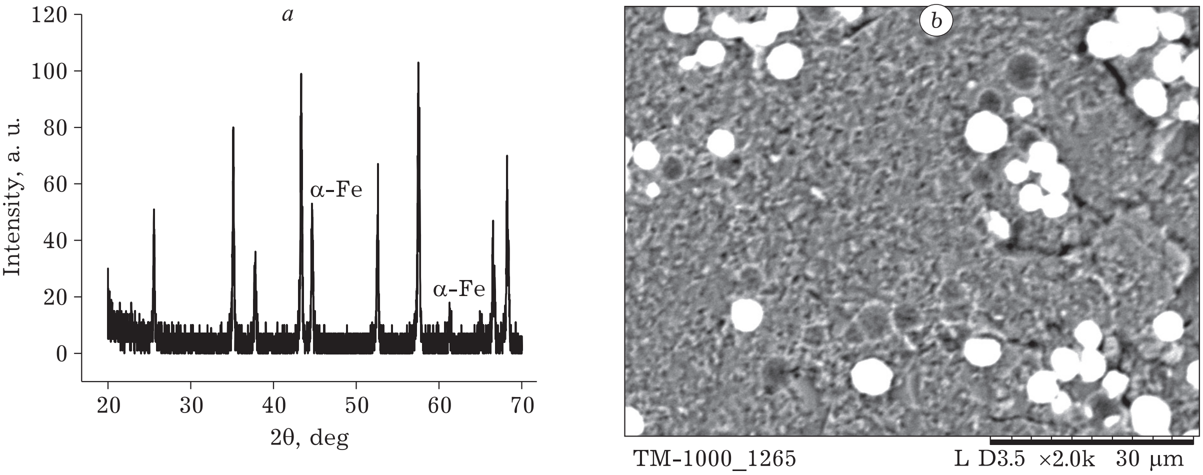

Fig. 6. X-ray diffraction pattern (a) and SEM image (b) of fracture surface of 5 % Fe_2O_3 containing sample after GIP (1525 °C) procedure.

during sintering is not sufficient to form through conductive paths, although the causes for such significant differences in electrical conductivity are not completely clear.

Figure 6 gives the X-ray diffraction pattern of the fracture surface, i.e. the inner region of the material exposed to GIP at 1525 °C, and Fig. 7 presents its SEM image. The X-ray diffraction pattern demonstrates alumina peaks without their position shifting caused by the introduction of iron cations into the lattice, and also the metallic α-iron peak. Spherical iron particles with a size of 3–5 μm are visible in the micrograph of alumina matrix. Thus, decomposition of the solid solution produced during air sintering and reduction of Fe_2O_3 to Fe takes place under these conditions.

In case of additional vacuum sintering of the samples at 1500 or 1600 °C, X-ray diffraction patterns of the outer surface of the material containing 3 or 5 % of Fe_2O_3 are similar to the data in Fig. 6, *i.e.* there are peaks of α-Al_2O_3 and α-Fe. At the same time, the inner regions do not contain the metal and alumina peaks are slightly shifted towards solution formation. The thickness of the outer layer under these conditions is about 150 μm (Fig. 7). Thus, Fe_2O_3 reduction process also proceeds under vacuum but less efficiently, since the oxygen partial pressure in the graphite furnace seems to be much lower than vacuum (10^{-6} Torr) and the internal areas are not affected.

Proceeding from the findings, the lack of prospects of using GIP procedure in a reducing medium to obtain the material with the required properties is obvious. Despite the homogeneity of spherical iron particles in the

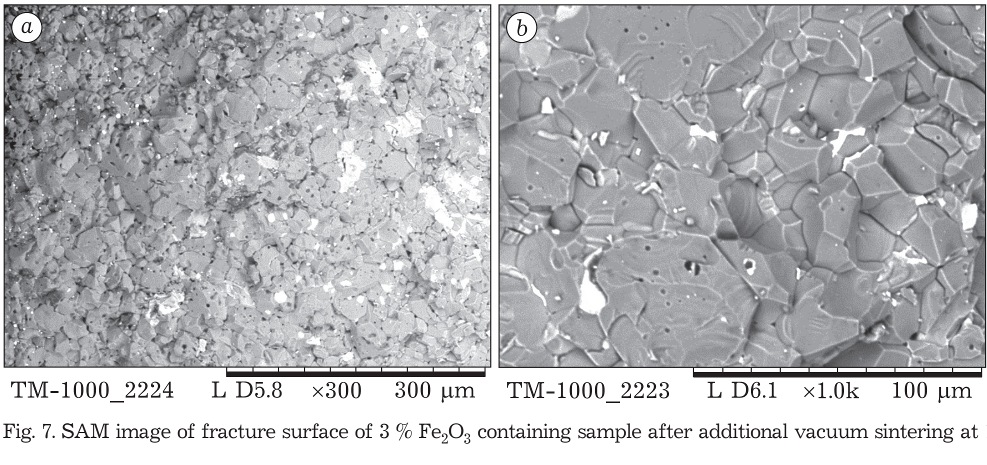

Fig. 7. SAM image of fracture surface of 3 % Fe_2O_3 containing sample after additional vacuum sintering at 1500 °C.

alumina matrix and a very thin microstructure, electrical conductivity of this composite will significantly exceed the required values in case of generating the closed three-dimensional metal grid.

At the same time, the inner areas of the vacuum-sintered material are not exposed to reduction. They almost do not have pores, unlike the outer layer, and may ensure full gas impermeability with the required conductivity level.

CONCLUSION

During air- two-component ultrafine powders sintering, it is possible to obtain two-phase material with a density of 93–94 % of the theoretically possible amounts that has electrical conductivity in the 10^{-8}–10^{-9} S/m range. The use of GIP procedure to the material leads to the reduction of Fe_2O_3 to Fe and therefore does not allow increasing matter density. The outer porous layer (150 μm) wherein the reduction process also proceeds is generated in the case of using vacuum sintering. However, inner regions are not affected and almost deprived of porosity.

Thus, prospects open up for further studies on vacuum sintering utilization with a view to obtaining materials that are conductive in the required range of materials with a larger density and hence with improved mechanical properties and gas impermeability.

Acknowledgements

The work was supported by RSF, the project No. 14-50-00080.

REFERENCES

1 Shutilov R. A., Myz A. L., Kuznetsov V. L., Karagedov G. R., *Perspekt. Mater.*, 2016, Vol. 8, P. 64–72. (in Rus.).
2 Ahmad K., Pan W., Shi S.-L., *Appl. Phys. Lett.*, 2006, Vol. 89, P. 133122.
3 Muan A., Gee C. L., *J. Amer. Ceram. Soc.*, 1956, Vol. 39, No. 6, P. 207–214.
4 Ito S., Yui Y., Mizuguchi J., *Mater. Transact.*, 2010, Vol. 51, No. 6, P. 1163–1167.
5 Karagedov G. R., Myz A. L., *J. Eur. Ceram. Soc.*, 2012, Vol. 32, P. 219–225.
6 Karagedov G. R., Myz A. L., Kichay O. V., *Chem. Sust. Dev.* [in Russian], 2016, Vol. 24, No. 2, P. 157–162.
7 Pat. RU No. 2392226, 2010.
8 Pat. RU No. 2625104, 2017.